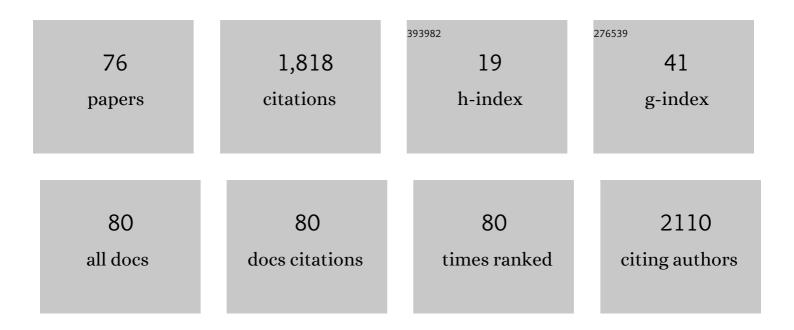
Byungki Ryu

List of Publications by Year in descending order

Source: https://exaly.com/author-pdf/2810363/publications.pdf Version: 2024-02-01



#	Article	IF	CITATIONS
1	Effect of microstructure on thermoelectric conversion efficiency in metastable Î ² -phase AgSbTe2. Acta Materialia, 2022, 222, 117443.	3.8	18
2	Off-Centered Pb Interstitials in PbTe. Materials, 2022, 15, 1272.	1.3	2
3	International Round Robin Test of Thermoelectric Generator Modules. Materials, 2022, 15, 1627.	1.3	6
4	Anomalous Optoelectric Properties of an Ultrathin Ruthenium Film with a Surface Oxide Layer for Flexible Transparent Conducting Electrodes. Advanced Functional Materials, 2022, 32, .	7.8	3
5	Understanding the dopability of p-type Mg ₂ (Si,Sn) by relating hybrid-density functional calculation results to experimental data. JPhys Energy, 2022, 4, 035001.	2.3	3
6	Neural network-assisted optimization of segmented thermoelectric power generators using active learning based on a genetic optimization algorithm. Energy Reports, 2022, 8, 6633-6644.	2.5	15
7	Unique temperature distribution and explicit efficiency formula for one-dimensional thermoelectric generators under constant Seebeck coefficients. Nonlinear Analysis: Real World Applications, 2022, 68, 103649.	0.9	1
8	Native point defects and low p-doping efficiency in Mg2(Si,Sn) solid solutions: A hybrid-density functional study. Journal of Alloys and Compounds, 2021, 853, 157145.	2.8	16
9	On the relevance of point defects for the selection of contacting electrodes: Ag as an example for Mg2(Si,Sn)-based thermoelectric generators. Materials Today Physics, 2021, 16, 100309.	2.9	19
10	Effect of defect interactions with interstitial Ag in the lattice of Bi <i>x</i> Sb2â^' <i>x</i> Te3 alloys and their thermoelectric properties. Applied Physics Letters, 2021, 118, .	1.5	8
11	Micromechanics-based theoretical prediction for thermoelectric properties of anisotropic composites and porous media. International Journal of Thermal Sciences, 2021, 165, 106918.	2.6	5
12	Regulating Te Vacancies through Dopant Balancing via Excess Ag Enables Rebounding Power Factor and High Thermoelectric Performance in pâ€7ype PbTe. Advanced Science, 2021, 8, e2100895.	5.6	18
13	Thermoelectric degrees of freedom determining thermoelectric efficiency. IScience, 2021, 24, 102934.	1.9	15
14	Entropy stabilized off-stoichiometric cubic γ-Cu1â^'xlx phase containing high-density Cu vacancies. AIP Advances, 2021, 11, .	0.6	3
15	Overcoming Asymmetric Contact Resistances in Al-Contacted Mg2(Si,Sn) Thermoelectric Legs. Materials, 2021, 14, 6774.	1.3	14
16	Structural Analysis, Phase Stability, Electronic Band Structures, and Electric Transport Types of (Bi2)m(Bi2Te3)n by Density Functional Theory Calculations. Applied Sciences (Switzerland), 2021, 11, 11341.	1.3	1
17	Dimension reduction of thermoelectric properties using barycentric polynomial interpolation at Chebyshev nodes. Scientific Reports, 2020, 10, 13456.	1.6	2
18	Counterintuitive example on relation between <i>ZT</i> and thermoelectric efficiency. Applied Physics Letters, 2020, 116, .	1.5	16

ΒΥUNGKI RYU

#	Article	IF	CITATIONS
19	Thermoelectric Properties of Off-Stoichiometric Bi2Te2Se Compounds. Journal of Electronic Materials, 2020, 49, 5308-5316.	1.0	4
20	Hybrid-Functional and Quasi-Particle Calculations of Band Structures of Mg2Si, Mg2Ge, and Mg2Sn. Journal of the Korean Physical Society, 2019, 75, 144-152.	0.3	20
21	Fine tuning of Fermi level by charged impurity-defect cluster formation and thermoelectric properties in n-type PbTe-based compounds. Journal of Materials Chemistry A, 2019, 7, 16488-16500.	5.2	24
22	Investigation of effective thermoelectric properties of composite with interfacial resistance using micromechanics-based homogenisation. International Journal of Heat and Mass Transfer, 2019, 144, 118620.	2.5	20
23	Highly anisotropic thermoelectric transport properties responsible for enhanced thermoelectric performance in the hot-deformed tetradymite Bi2Te2S. Journal of Alloys and Compounds, 2019, 783, 448-454.	2.8	15
24	Antimony-induced heterogeneous microstructure of Mg2Si0.6Sn0.4 thermoelectric materials and their thermoelectric properties. Journal of Alloys and Compounds, 2018, 739, 129-138.	2.8	13
25	Work function of bismuth telluride: First-principles approach. Journal of the Korean Physical Society, 2018, 72, 122-128.	0.3	16
26	Enhancing Thermoelectric Performances of Bismuth Antimony Telluride via Synergistic Combination of Multiscale Structuring and Band Alignment by FeTe ₂ Incorporation. ACS Applied Materials & Interfaces, 2018, 10, 3689-3698.	4.0	66
27	Control of Carrier Concentration by Ag Doping in N-Type Bi2Te3 Based Compounds. Applied Sciences (Switzerland), 2018, 8, 735.	1.3	14
28	A micromechanics-based analytical solution for the effective thermal conductivity of composites with orthotropic matrices and interfacial thermal resistance. Scientific Reports, 2018, 8, 7266.	1.6	27
29	Abnormal Optoelectric Properties of Two-Dimensional Protonic Ruthenium Oxide with a Hexagonal Structure. ACS Applied Materials & Interfaces, 2018, 10, 22661-22668.	4.0	7
30	Defect chemistry and enhancement of thermoelectric performance in Ag-doped Sn _{1+δâ´`x} Ag _x Te. Journal of Materials Chemistry A, 2017, 5, 2235-2242.	5.2	54
31	Quasi-High-Pressure Effects in Transition-Metal-Rich Dichalcogenide, Hf ₃ Te ₂ . Journal of Physical Chemistry C, 2017, 121, 25541-25546.	1.5	1
32	Thermoelectric power factor of Bi-Sb-Te and Bi-Te-Se alloys and doping strategy: First-principles study. Journal of Alloys and Compounds, 2017, 727, 1067-1075.	2.8	16
33	Enhanced thermoelectric properties of AgSbTe2 obtained by controlling heterophases with Ce doping. Scientific Reports, 2017, 7, 4496.	1.6	29
34	GW Calculations Overcoming DFT Band Gap Problem. Physics and High Technology, 2017, 26, 15-21.	0.1	0
35	Enhancement of the thermoelectric figure of merit in n-type Cu0.008Bi2Te2.7Se0.3 by using Nb doping. Journal of the Korean Physical Society, 2016, 68, 7-11.	0.3	1
36	Hybrid-density functional theory study on the band structures of tetradymite-Bi2Te3, Sb2Te3, Bi2Se3, and Sb2Se3 thermoelectric materials. Journal of the Korean Physical Society, 2016, 69, 1683-1687.	0.3	27

Βγυνςκι Ryu

#	Article	lF	CITATIONS
37	Thermoelectric properties of Bi2Te2.7Se0.3 nanocomposites embedded with MgO nanoparticles. Journal of the Korean Physical Society, 2016, 69, 1314-1320.	0.3	4
38	Effect of La-doping on AgSbTe2 thermoelectric compounds. Journal of the Korean Physical Society, 2016, 68, 164-169.	0.3	5
39	Fabrication of Miniature Thermoelectric Generators Using Bulk Materials. Journal of Electronic Materials, 2016, 45, 3453-3459.	1.0	2
40	Importance of crystal chemistry with interstitial site determining thermoelectric transport properties in pavonite homologue Cu–Bi–S compounds. CrystEngComm, 2016, 18, 1453-1461.	1.3	14
41	Prediction of the band structures of Bi2Te3-related binary and Sb/Se-doped ternary thermoelectric materials. Journal of the Korean Physical Society, 2016, 68, 115-120.	0.3	30
42	Enhanced thermoelectric properties and development of nanotwins in Na-doped Bi0.5Sb1.5Te3 alloy. Electronic Materials Letters, 2016, 12, 290-295.	1.0	17
43	Computational Simulations of Thermoelectric Transport Properties. Journal of the Korean Ceramic Society, 2016, 53, 273-281.	1.1	52
44	Deposition of <i>n</i> -Type Bi ₂ Te ₃ Thin Films on Polyimide by Using RF Magnetron Co-Sputtering Method. Journal of Nanoscience and Nanotechnology, 2015, 15, 8299-8304.	0.9	15
45	Enhanced thermoelectric performance of n-type Cu _{0.008} Bi ₂ Te _{2.7} Se _{0.3} by band engineering. Journal of Materials Chemistry C, 2015, 3, 10604-10609.	2.7	34
46	Defects responsible for abnormal <i>n</i> -type conductivity in Ag-excess doped PbTe thermoelectrics. Journal of Applied Physics, 2015, 118, .	1.1	17
47	Electronic Structures and Seebeck Coefficients of Bi ₂ Te ₃ , Sb ₂ Te ₃ , and (Bi _{0.} ₂₅ Sb _{0.} 75) ₂ Te ₃ : A First-Principles Calculation Study. Journal of Nanoelectronics and Optoelectronics, 2015, 10, 391-396.	0.1	4
48	Origin of High Photoconductive Gain in Fully Transparent Heterojunction Nanocrystalline Oxide Image Sensors and Interconnects. Advanced Materials, 2014, 26, 7102-7109.	11.1	65
49	Action-derived molecular dynamics simulations for the migration and coalescence of vacancies in graphene and carbon nanotubes. Journal of Physics Condensed Matter, 2014, 26, 115303.	0.7	4
50	Nonlocal Problems Arising in Thermoelectrics. Mathematical Problems in Engineering, 2014, 2014, 1-7.	0.6	4
51	Enhancement of thermoelectric properties of Mg2Si compounds with Bi doping through carrier concentration tuning. Electronic Materials Letters, 2014, 10, 807-811.	1.0	16
52	Electronic Structure and X-ray Absorption Spectra of Rutile TiO2 Using First-Principles Calculations. Journal of Korean Institute of Metals and Materials, 2014, 52, 1025-1029.	0.4	0
53	Substantial enhancement in intrinsic coercivity on M-type strontium hexaferrite through the increase in magneto-crystalline anisotropy by co-doping of group-V and alkali elements. Applied Physics Letters, 2013, 103, 242417.	1.5	11
54	Cu–Bi–Se-based pavonite homologue: a promising thermoelectric material with low lattice thermal conductivity. Journal of Materials Chemistry A, 2013, 1, 9768.	5.2	13

ΒΥUNGKI RYU

#	Article	IF	CITATIONS
55	Enhancement of the Thermoelectric Performance of Bi0.4Sb1.6Te3 Alloys by In and Ga Doping. Journal of Electronic Materials, 2013, 42, 1617-1621.	1.0	24
56	Rational design of Nb-based alloys for hydrogen separation: A first principles study. AIP Advances, 2013, 3, .	0.6	2
57	Metal Oxide Thin Film Phototransistor for Remote Touch Interactive Displays. Advanced Materials, 2012, 24, 2631-2636.	11.1	143
58	Ab initio study of boron segregation and deactivation at Si/SiO2 interface. Microelectronic Engineering, 2012, 89, 120-123.	1.1	16
59	First-principles study of Si CMOS materials and nanostructures. , 2011, , .		0
60	Electronic structure of oxygen-vacancy defects in amorphous In-Ga-Zn-O semiconductors. Physical Review B, 2011, 84, .	1.1	253
61	Stability of Donor-Pair Defects in Si _{1–<i>x</i>} Ge _{<i>x</i>} Alloy Nanowires. Journal of Physical Chemistry C, 2011, 115, 10345-10350.	1.5	7
62	The Electronic Structure of Oxygen Vacancy in Amorphous HfSiO[sub 4]. , 2011, , .		0
63	Electronic Structure of O-vacancy in Amorphous Zinc-Tin Oxides. , 2011, , .		0
64	Hole Gas Induced by Defects in Geâ^•Si Core-Shell Nanowires. , 2011, , .		2
65	Electronic Structure of O-vacancy in High-k Dielectrics and Oxide Semiconductors. Materials Research Society Symposia Proceedings, 2011, 1370, 3.	0.1	0
66	O-vacancy as the origin of negative bias illumination stress instability in amorphous In–Ga–Zn–O thin film transistors. Applied Physics Letters, 2010, 97, .	1.5	380
67	Defects responsible for the Fermi level pinning in n+ poly-Si/HfO2 gate stacks. Applied Physics Letters, 2010, 97, .	1.5	7
68	Defects Responsible for the Hole Gas in Ge/Si Coreâ^'Shell Nanowires. Nano Letters, 2010, 10, 116-121.	4.5	49
69	Electronic structure of oxygen vacancy in crystalline InGaO3(ZnO)m. Physica B: Condensed Matter, 2009, 404, 4794-4796.	1.3	27
70	The electronic properties of the interface structure between ZnO and amorphous HfO2. Physica B: Condensed Matter, 2009, 404, 4823-4826.	1.3	7
71	Local bonding effect on the defect states of oxygen vacancy in amorphous HfSiO4. Applied Physics Letters, 2009, 95, 082905.	1.5	4
72	First-principles Study of the Electronic Structure of CrystallineInGaO\$_{ m 3}\$(ZnO)\$_{ m 3}\$. Journal of the Korean Physical Society, 2009, 55, 112-115.	0.3	1

ΒΥUNGKI **R**YU

#	Article	IF	CITATIONS
73	Structural and electronic properties of crystalline InGaO3(ZnO)m. Applied Physics Letters, 2008, 93, 111901.	1.5	22
74	Effect of atomic-scale defects on the low-energy electronic structure of graphene: Perturbation theory and local-density-functional calculations. Physical Review B, 2008, 77, .	1.1	45
75	Crystal binding and metal-semiconductor transition in aluminate nanotube bundles. Physical Review B, 2007, 75, .	1.1	1
76	First-principles study of the electronic structure of aluminate nanotubes. Journal of Physics: Conference Series, 2007, 61, 195-199.	0.3	0